Enhancement of α-particle formation near ^{100}Sn

Clark, R. M.; Macchiavelli, A. O.; Crawford, H. L.; Fallon, P.; Rudolph, D.; Såmark-Roth, A.; Campbell, C. M.; Cromaz, M.; Morse, C.; Santamaria, C.

Published in:
Physical Review C

DOI:
10.1103/PhysRevC.101.034313

2020

Document Version:
Publisher's PDF, also known as Version of record

Enhancement of α-particle formation near ^{100}Sn

R. M. Clark,[1] A. O. Macchiavelli,[1] H. L. Crawford,[1] P. Fallon,[1] D. Rudolph,[2] A. Såmark-Roth,[2] C. M. Campbell,[1] M. Cromaz,[1] C. Morse,[1] and C. Santamaria[1]

[1]*Nuclear Science Division, Lawrence Berkeley National Laboratory, Berkeley, California 94720, USA*

[2]*Department of Physics, Lund University, 22100 Lund, Sweden*

(Received 24 July 2019; revised manuscript received 18 January 2020; accepted 11 February 2020; published 27 March 2020)

The superfluid tunneling model is applied to the calculation of ground-state–to–ground-state α decay in the even-even neutron-deficient Te-Ba nuclei. We show that there is a larger α-particle formation probability in nuclei of this region above ^{100}Sn when compared to analogous nuclei above ^{208}Pb. This is consistent with the expected systematic variation of the pair gap Δ as a function of mass number. The recent experimental data on the α decay of the $N = Z$ nuclei ^{104}Te and ^{108}Xe are shown to leave open the possibility of enhanced α-particle formation involving nucleon correlations beyond the standard treatment of like-nucleon pairing, which is the mechanism suggested as underlying "superallowed" α decay.

DOI: 10.1103/PhysRevC.101.034313

I. INTRODUCTION

A region of "superallowed" α decay in the neutron-deficient Te-Ba nuclei was first suggested over fifty years ago [1]. It was thought that the interactions between protons and neutrons occupying similar single-particle orbitals could enhance α-particle formation. One would expect this effect to be greatest for $N = Z$ nuclei, when the protons and neutrons occupy identical orbitals. This would lead to significantly increased α-decay widths in nuclei just above doubly magic ^{100}Sn ($N = Z = 50$) when compared to those in analogous nuclei just above doubly magic ^{208}Pb ($N = 126$, $Z = 82$). This prediction seems to have been borne out with the recent observation of the $^{108}\text{Xe} \rightarrow {}^{104}\text{Te} \rightarrow {}^{100}\text{Sn}$ decay chain, where, on the basis of two observed events, it was concluded that the reduced α width for at least one of either ^{108}Xe or ^{104}Te must be more than a factor of 5 larger than that for ^{212}Po [2]. From comparison to the available experimental data on these nuclei, and other nearby isotopes of Te, Xe, and Ba [3–12], we can now start to examine the evolution of α decay in this region and try to understand effects such as the role of proton-neutron interactions in the α-particle formation.

The theory of α decay was initially formulated in 1928 by Gamow [13], and independently by Gurney and Condon [14], who described the process as a tunneling of the preformed α particle through a Coulomb barrier. There have been many subsequent efforts towards developing a quantitative description of α decay involving calculations of both the α-particle formation probability and the barrier penetrability (see, for example, Refs. [15–17] and references therein). There have even been recent attempts to calculate and compare the structure and α-particle formation of ^{212}Po and ^{104}Te using fully microscopic methods [18,19]. In this paper we take a more phenomenological approach, trying to qualitatively understand the role of pairing correlations in the formation of α particles in nuclei above ^{100}Sn and ^{208}Pb.

The model we will use is the superfluid tunneling model (STM) as described in [20]. The model has been successfully applied to calculations of particle emission including α decay and cluster radioactivity [21–23]. Recently, it was shown that the STM could be applied to the description of α-decaying ground states, and multiquasiparticle states, across different regions of the nuclear chart from the neutron-deficient $A \approx 150$ region [24] up through the heavy actinide region [25]. In another study [26] we applied the STM to compare with the experimental data on all known even-even superheavy nuclei (SHN) with $100 \leqslant Z \leqslant 118$. A remarkable quantitative agreement, comparable to the fits of recent empirical parametrizations, was found. Experimental α-decay half lives, for even-even ground states, have been reproduced to within a factor of 3 for nuclei with $A \geqslant 150$ [24–26].

The STM involves the nucleus evolving to a clusterlike configuration, which, in the case of α decay, comprises a touching configuration of the daughter nucleus and α particle. The subsequent decay process is described in terms of standard Gamow theory of tunneling through a barrier. The importance of nuclear structure on clustering and the α-decay process has been noted before [27]. For the STM, the evolution of the parent nucleus to the clusterlike configuration is dominated by pairwise rearrangements of nucleons, which occur under the action of the residual nuclear interaction, which is dominated by pairing. The STM enables us to examine effects arising from changes in the residual interaction and the influence these changes have on the α-formation factor.

In previous articles [24–26] the model has been discussed in detail. For completeness, we describe the main features of the STM in the Appendix. In Sec. II we compare the results of our calculations, using the STM, to the experimental data on the α decays of even-even nuclei just above ^{100}Sn. We

TABLE I. The half lives of the known α decays from the ground states of even-even nuclei near ^{100}Sn, $T_{1/2,\mathrm{expt}}(\alpha)$ in seconds. The experimentally measured total half lives and branching ratios are taken into account. The third column gives the energy of the α decay E_α in MeV. The fourth gives the decimal logarithm of the experimental half life, which can be compared to the values calculated using the empirical parametriztion of Royer and the STM, as discussed in the text, which are given in the fifth and sixth columns, respectively. The seventh column gives the value of the pairing gap, Δ_{fit}, in MeV, that must be used in the STM in order to reproduce the experimental half life. The eighth column gives the calculated α-formation probability P, corresponding to the fitted lifetimes.

Nucleus	$T_{1/2,\mathrm{expt}}(\alpha)$ (s)	E_α (MeV)	$\log_{10}(T_{1/2,\mathrm{expt}})$ (s)	$\log_{10}(T_{1/2,\mathrm{Royer}})$ (s)	$\log_{10}(T_{1/2,\mathrm{STM}})$ (s)	Δ_{fit} (MeV)	P ($\times 10^{-2}$)
^{114}Ba	42^{+25}_{-18} [6]	3.480(20) [6]	$1.62^{+0.21}_{-0.24}$	$2.21^{+0.14}_{-0.13}$	$1.98^{+0.14}_{-0.13}$	$1.74^{+0.39}_{-0.28}$	$1.74^{+1.63}_{-0.89}$
^{112}Xe	338^{+475}_{-234} [7,8]	3.216(7) [7]	$2.53^{+0.38}_{-0.51}$	$2.74^{+0.05}_{-0.05}$	$2.54^{+0.05}_{-0.05}$	$1.49^{+0.46}_{-0.24}$	$0.98^{+1.70}_{-0.55}$
^{110}Xe	$0.148^{+0.090}_{-0.087}$ [6]	3.720(20) [6]	$-0.83^{+0.21}_{-0.38}$	$-0.52^{+0.11}_{-0.12}$	$-0.71^{+0.11}_{-0.12}$	$1.58^{+0.47}_{-0.20}$	$1.36^{+1.95}_{-0.60}$
^{108}Xe	$58^{+106}_{-23} \times 10^{-6}$ [2]	4.4(2) [2]	$-4.25^{+0.46}_{-0.21}$	$-4.01^{+0.96}_{-0.89}$	$-4.14^{+0.94}_{-0.88}$	$1.58^{+1.72}_{-0.63}$	$1.56^{+8.43}_{-1.43}$
^{110}Te	$2.78(12) \times 10^{6}$ [9,10]	2.624(15) [9]	$6.44^{+0.02}_{-0.02}$	$6.23^{+0.15}_{-0.14}$	$6.06^{+0.15}_{-0.14}$	$1.27^{+0.09}_{-0.07}$	$0.43^{+0.17}_{-0.12}$
^{108}Te	4.3(4) [7,8,11]	3.314(4) [11]	$0.63^{+0.04}_{-0.04}$	$0.75^{+0.03}_{-0.03}$	$0.58^{+0.03}_{-0.03}$	$1.47^{+0.04}_{-0.05}$	$1.00^{+0.14}_{-0.12}$
^{106}Te	$70^{+20}_{-15} \times 10^{-6}$ [6,7,12]	4.128(9) [7]	$-4.15^{+0.10}_{-0.11}$	$-3.85^{+0.04}_{-0.04}$	$-3.97^{+0.04}_{-0.04}$	$1.66^{+0.13}_{-0.12}$	$1.98^{+0.57}_{-0.46}$
^{104}Te	$<18 \times 10^{-9}$ [2]	4.9(2) [2]	<-7.74	$-7.10^{+0.74}_{-0.70}$	$-7.14^{+0.76}_{-0.69}$	>1.47	>1.65

show that there is a larger α-particle formation probability in nuclei of this region, when compared to analogous nuclei above ^{208}Pb. However, this is shown to be consistent with the expectations of the systematic variation of the pair gap Δ as a function of mass number A. In Sec. III we examine the recent experimental data on the α decay of the $N = Z$ nuclei ^{104}Te and ^{108}Xe, which are shown to leave open the possibility of enhanced α-particle formation involving pairing correlations beyond the standard treatment of like-nucleon isovector pairing. Such a mechanism has been suggested as underlying superallowed α decay. This will be followed by a short summary.

II. ALPHA DECAYS IN EVEN-EVEN NUCLEI NEAR ^{100}Sn

Using the STM as discussed above and described in the Appendix, we have calculated the ground-state–to–ground-state decays for the known α-decaying even-even nuclei in the ^{100}Sn region. The results are presented in Table I. For comparison, we have also calculated the ground-state–to–ground-state decays for "analogous" nuclei in the ^{208}Pb region. The results are presented in Table II. By analogous we mean the nuclei have the same type and number of nucleons beyond the closed shell reference nucleus. For instance, we would call ^{214}Po analogous to ^{106}Te since they both have an additional two protons and four neutrons outside the doubly magic core nuclei of ^{208}Pb and ^{100}Sn, respectively.

In order to perform the STM calculations we must estimate the pair gap Δ, which is used as an input. The pair gap has long been known [29] to show a smooth decrease with increasing atomic mass number A, and there are different expressions which aim at reproducing the empirical pair gaps extracted from multipoint mass-difference formulas [30]. In particular, we have considered an expression of the form

$$\Delta = \left\{ a - b\left[\frac{(N-Z)}{A}\right]^2 \right\} A^{-1/3}. \tag{1}$$

This equation was originally proposed in [31] with fit parameters of $a = 7.2$ MeV and $b = 44$ MeV. To see how well the STM reproduces the data using this parametrization for Δ, one can compare the values of the decimal logarithms in columns 4–6 of Tables I and II. Note that the fifth column of both Tables I and II are the predictions from the empirically fitted formula of Royer [32], $T_{1/2,\mathrm{Royer}}$. The errors in the calculated half lives, for $T_{1/2,\mathrm{Royer}}$ and $T_{1/2,\mathrm{STM}}$, reflect the uncertainty in the α-decay energies E_α. One clearly sees that the experimental data are reproduced rather well by both the Royer formula and the STM calculation. A difference in decimal logarithm of ± 0.477 would correspond to a factor-of-3 difference between the experimental and theoretical half lives. Generally, the data and calculation agree to within that difference and, on this basis, one would suggest that there is nothing unusual about the α decay in the region above ^{100}Sn. In the STM, the experimental values are described within typical uncertainties once the systematic variation of the pair gap, as expressed in Eq. (1), is taken into account.

One can look at the problem in reverse and use the STM in order to extract estimates of the pair gap. Tables I and II present, in the seventh column, the values of the pair gaps,

TABLE II. Same as Table I, but for some of the known ground-state α decays of nuclei above ^{208}Pb. All the data are taken from [28]. Experimental errors are small enough to be ignored when considering the extracted values of $\Delta_{\rm fit}$ and P.

Nucleus	$T_{1/2,\rm expt}(\alpha)$ (s)	E_α (MeV)	$\log_{10}(T_{1/2,\rm expt})$ (s)	$\log_{10}(T_{1/2,\rm Royer})$ (s)	$\log_{10}(T_{1/2,\rm STM})$ (s)	$\Delta_{\rm fit}$ (MeV)	P ($\times 10^{-2}$)
^{222}Ra	38.0(5)	6.588(5)	1.58	1.81	1.87	0.97	0.30
^{220}Ra	$18(2)\times 10^{-3}$	7.453(7)	−1.74	−1.45	−1.53	0.97	0.39
^{220}Rn	55.6(1)	6.288 08(10)	1.75	2.11	2.24	1.00	0.38
^{218}Rn	$33.75(15)\times 10^{-3}$	7.1292(12)	−1.47	−1.14	−1.10	0.99	0.45
^{216}Rn	$45(5)\times 10^{-6}$	8.050(10)	−4.35	−4.09	−4.09	0.98	0.55
^{218}Po	185.8(7)	6.002 35(9)	2.27	2.43	2.73	0.94	0.29
^{216}Po	0.145(2)	6.7783(5)	−0.84	−0.72	−0.53	0.93	0.33
^{214}Po	$1.64(2)\times 10^{-4}$	7.686 82(7)	−3.78	−3.78	−3.67	0.90	0.36
^{212}Po	$0.299(2)\times 10^{-6}$	8.784 86(12)	−6.52	−6.83	−6.74	0.82	0.32

$\Delta_n = \Delta_p = \Delta_{\rm fit}$, that give the transition matrix element v in Eq. (A3) of the Appendix, such that the STM reproduces the experimental half lives. It can be seen immediately that the fitted pair gaps for all the nuclei in the Te-Ba region are significantly higher than the values of Δ extracted for nuclei in the Po-Ra region. This, in turn, leads to significantly higher values for the extracted α-particle formation probabilities P, which are given in the eighth columns of Tables I and II. In Fig. 1, we show the variation of P as one approaches the $N = Z$ line along either an isotonic ($N = 58$) or isotopic (Te) chain. A rise in P is seen in the plots indicating that the ease of forming an α particle increases as one moves towards the $N = Z$ line. For comparison we also show the values for analogous nuclei above ^{208}Pb, namely the $N = 134$ isotones ^{222}Ra, ^{220}Rn, and ^{218}Po, and along the Po isotopes ^{214}Po, ^{216}Po, and ^{218}Po. One does not see a commensurate rise in P for these nuclei. However, we again should point out that the large values of the α-particle formation probabilities P in nuclei just above ^{100}Sn, along with the observed increase in P as one approaches $N = Z$, are in line with *a priori* expectations of the systematic variation of the pair gap given by Eq. (1). There is very little evidence for enhanced neutron-proton pairing correlations, which is the mechanism suggested for superallowed α decay.

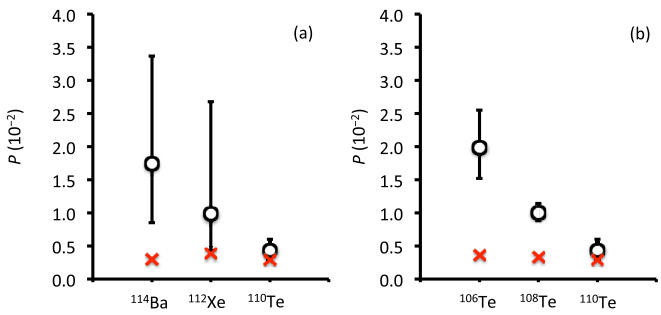

FIG. 1. Plots of the variation of the α-particle formation probabilities P along (a) the $N = 58$ isotonic chain, and along (b) the Te isotopic chain (open circles). The values of P are taken from Table I. The rise in P as one approaches the $N = Z$ line is clearly seen. The red crosses are values of P for the analogous nuclei above ^{208}Pb, by which we mean the same type and number of nucleons beyond the closed shells, namely in (a) the N = 134 isotones ^{222}Ra, ^{220}Rn, and ^{218}Po, and in (b) the Po isotopic chain ^{214}Po, ^{216}Po, and ^{218}Po.

If there are enhanced pairing correlations at play in nuclei of the ^{100}Sn region then the effect will be greatest for $N = Z$ nuclei when the protons and neutrons occupy the same orbitals. Therefore, we now turn to a careful reexamination of the recent experimental data on the α decay of the $N = Z$ nuclei ^{104}Te and ^{108}Xe [2].

III. ALPHA DECAY OF $N = Z$ NUCLEI ^{108}Xe AND ^{104}Te

The first observation of the $^{108}\text{Xe} \rightarrow {}^{104}\text{Te} \rightarrow {}^{100}\text{Sn}$ α-decay sequence was recently reported [2]. The results were based on the unambiguous identification of only two events that were sufficient to allow determination of the α-decay energies and half lives of ^{108}Xe [$E_\alpha = 4.4(2)$ MeV and $T_{1/2} = 58^{+106}_{-23}$ μs] and ^{104}Te [$E_\alpha = 4.9(2)$ MeV and $T_{1/2} < 18$ ns]. These values were used in Table I. While the individual α-decay energies have large uncertainty, their sum is better constrained to give a value of 9.3(1) MeV. This information, along with some additional physical inferences, is sufficient to place significant constraints on the α-particle formation probabilities.

Figure 2 is an exclusion plot showing limits for the pair gaps, $\Delta(^{104}\text{Te})$ and $\Delta(^{108}\text{Xe})$, which are extracted using the STM in order to reproduce possible values of the half lives of ^{104}Te and ^{108}Xe. The points with horizontal error bars are the values for $\Delta(^{108}\text{Xe})$ extracted from the STM in order to reproduce the half life of $T_{1/2} = 58^{+106}_{-23}$ μs, while the extracted value of $\Delta(^{104}\text{Te})$ corresponds to a half life of $T_{1/2} = 18$ ns. Different possible values of the α-decay energies for ^{108}Xe, with the additional constraint on the sum energy mentioned above, are assumed. The experimental lower limit of $E_\alpha = 4.2$ MeV on the α-decay energy of ^{108}Xe gives the dashed horizontal line at about 1.5 MeV. Since the half life for the ^{104}Te decay is an upper limit, the extracted values of $\Delta(^{104}\text{Te})$ will all be lower limits. We then have assumed that the sum energy lies at the limit of the reported errors which gives the curve marked $\sum E_\alpha = 9.4$ MeV. Physical values of $\Delta(^{104}\text{Te})$ and $\Delta(^{108}\text{Xe})$ most likely lie above this curve.

One can then use some physical insights to place additional constraints on the pair gaps. While being close to doubly

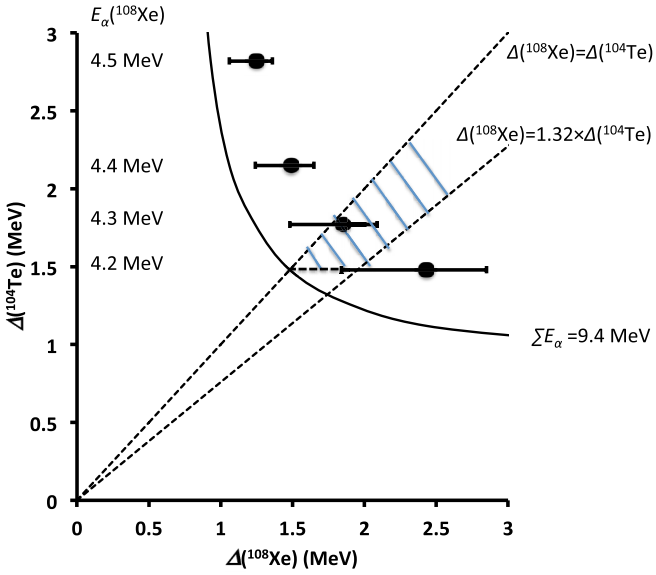

FIG. 2. An exclusion plot showing limits for the pair gaps, $\Delta(^{104}\mathrm{Te})$ and $\Delta(^{108}\mathrm{Xe})$, which are extracted using the STM in order to reproduce possible values of the half lives of ^{104}Te and ^{108}Xe. The filled circles with horizontal error bars are the values for $\Delta(^{108}\mathrm{Xe})$ extracted from the STM in order to reproduce the half life of $T_{1/2} = 58^{+106}_{-23}$ μs, while the extracted value of $\Delta(^{104}\mathrm{Te})$ corresponds to a half life of $T_{1/2} = 18$ ns, and is therefore a lower limit. Different possible values of the ^{108}Xe α-decay energy, $E_\alpha(^{108}\mathrm{Xe})$, are indicated to the left, with an additional constraint on the sum energy being assumed; the filled circles assume $\sum E_\alpha = 9.3$ MeV, while the solid curve indicates the range of possible $\Delta(^{108}\mathrm{Xe})$ values assuming $\sum E_\alpha = 9.4$ MeV. The additional constraint requiring that $\Delta(^{108}\mathrm{Xe}) > \Delta(^{104}\mathrm{Te})$ and the special limiting case treating the problem as a pure pairing force in a single-j shell, such that $\Delta(^{108}\mathrm{Xe}) = 1.32 \times \Delta(^{104}\mathrm{Te})$, are indicated with the dashed lines. The resulting region of allowed values of $\Delta(^{104}\mathrm{Te})$ and $\Delta(^{108}\mathrm{Xe})$ is indicated by the shaded hash marks. The region extends to higher values beyond the edges of the plot.

magic ^{100}Sn, we know that the transition to the superconducting phase happens rather quickly [33]. Thus, a BCS estimate, as discussed below, is justified to set some limits. First, BCS theory would suggest that $\Delta(^{108}\mathrm{Xe})$ must be larger than $\Delta(^{104}\mathrm{Te})$. Therefore, possible solutions must lie to the right of the $\Delta(^{108}\mathrm{Xe}) = \Delta(^{104}\mathrm{Te})$ line as shown in Fig. 2. Moreover, a maximum for the ratio of $\Delta(^{108}\mathrm{Xe})/\Delta(^{104}\mathrm{Te})$ is estimated by assuming the special case of a pure pairing force in a single-j shell. The gap in such a model is then given by [34]

$$\Delta = G\sqrt{\frac{n}{2}\left(\Omega - \frac{n}{2}\right)}, \tag{2}$$

where n is the number of particles and $\Omega = (2j+1)/2$ is the effective degeneracy of the shell. For ^{108}Xe (^{104}Te), $n = 4$ ($n = 2$), while $\Omega = 16$, corresponding to the shell spanning $N = 50$ to $N = 82$, resulting in the ratio of $\Delta(^{108}\mathrm{Xe})/\Delta(^{104}\mathrm{Te}) = 1.32$. Following the above reasoning leaves the shaded area in Fig. 2 as the region of physically allowed values of $\Delta(^{104}\mathrm{Te})$ and $\Delta(^{108}\mathrm{Xe})$. Note that the Δ_{VJH} values ≈ 1.5 MeV for both ^{104}Te and ^{108}Xe are barely contained within the shaded region. Therefore, the possibility remains that there is enhanced α-particle formation in these $N = Z$ nuclei just above ^{100}Sn.

IV. SUMMARY AND CONCLUSIONS

To recap, we have shown in the preceding sections that the α-particle formation probability is significantly larger in nuclei just above ^{100}Sn when compared to nuclei just above ^{208}Pb. However, following the suggestion that the pairing force is responsible for the α-particle formation, these larger formation probabilities are in line with *a priori* expectations of the systematic variation of the pairing gap. For the cases of the $N = Z$ nuclei, ^{104}Te and ^{108}Xe, the recent experimental evidence leaves open the possibility of superallowed α decay involving enhanced α-particle formation. This may arise in these self-conjugate nuclei, with protons and neutrons occupying identical single-particle orbitals, when neutron-proton pairing correlations, of both the isovector ($T = 1$) and/or isoscalar ($T = 0$) type, may occur. The competition between these two types of neutron-proton pairing has been a topic of considerable debate [35] but it has been shown that there is very little evidence for $T = 0$ neutron-proton-pairing condensation in the ground states of $N = Z$ nuclei [36]. However, it has been suggested that the isovector neutron-proton pairing can give rise to a condensate of α-like quartets, formed from the coupling of two isovector neutron-proton pairs, in the ground states of $N = Z$ nuclei above ^{100}Sn [37]. At some point, we may be able to see clear evidence of such an effect in the enhancement of the α-particle formation probability in the $N = Z$ nuclei just above ^{100}Sn. In such a scenario, the ground states of ^{104}Te and ^{108}Xe could be associated with one- and two-phonon α-like pairing vibrational states [38].

For the future, the highest priority should be to gather higher statistics data on the α decays of ^{104}Te and ^{108}Xe and to extend the experimental studies to heavier $N = Z$ nuclei like ^{112}Ba. Accurate values of decay energies and half lives will allow better estimates of the enhancement of α-particle formation and help constrain studies, such as this one, which aim to understand the role of nucleon-nucleon interactions in α-particle formation.

ACKNOWLEDGMENTS

This work has been supported, in part, by the U.S. DoE under Contract No. DE-AC02-05CH11231 (LBNL) and by the Knut and Alice Wallenberg Foundation (KAW 2015.0021). One of us (R.M.C.) would like to thank D. Clark for her continued support and encouragement.

APPENDIX: SUPERFLUID TUNNELING MODEL

The Hamiltonian of the STM can be written as

$$\left(\frac{\hbar^2}{2D}\frac{\partial^2}{\partial\xi^2} + V(\xi)\right)\psi(\xi) = E\psi(\xi). \tag{A1}$$

ξ is a generalized deformation variable describing the path of the system in the multidimensional space of deformations.

In the case of only quadrupole deformation, this would mean that ξ is proportional to the axial deformation parameter β_2. The parent nucleus evolves from a configuration with a small deformation, $\xi \approx 0$, to the touching configuration of daughter-plus-α particle defined to be at $\xi = 1$.

Equation (1) can be discretized on a mesh of n steps such that for each step $\Delta\xi = 1/n$. One can then derive the expression for the inertial mass parameter as

$$D = -\frac{\hbar^2}{2v}n^2. \tag{A2}$$

v is the transition matrix element between two successive steps. For α decay, $n = 4$ is assumed [20,23]. The transition matrix element is governed by the pairing operator and is estimated using the Bardeen-Cooper-Schrieffer (BCS) model to be

$$v = -\left(\frac{\Delta_n^2 + \Delta_p^2}{4G}\right). \tag{A3}$$

$G = 25/A$ MeV is the standard pairing strength and $\Delta_n = \Delta_p = \Delta$ are the pair gap parameters.

The decay constant λ can be calculated in terms of the α-particle formation probability, P, the assault frequency of the particle against the barrier (also known as the knocking frequency), f, and the transmission coefficient of the α particle through the barrier, T, such that

$$\lambda = PfT. \tag{A4}$$

To calculate P we use the wave function of the ground state of a harmonic oscillator such that $P = |\psi(\xi = 1)|^2$ with

$$\psi(\xi) = \left(\frac{\alpha}{\sqrt{\pi}}\right)^{1/2} e^{-(1/2)\alpha^2\xi^2}, \tag{A5}$$

where

$$\alpha^2 = \sqrt{\frac{C}{2|v|}}n. \tag{A6}$$

The potential energy parameter is $C = 2V(\xi = 1) = 2(V_N + V_C - Q_\alpha)$ with V_N and V_C being the nuclear potential (for which we used the Christensen-Winther potential [39]) and the Coulomb potential, respectively. Q_α is the Q value for the specific α-decay transition being considered and is determined from the experimentally measured α-decay energy E_α. The details of the potential parameters used can be found in [39]. The assault frequency can then be calculated via the formula $f = \omega/2\pi$, where $\omega = \sqrt{C/D}$.

Finally, the transmission coefficient T_L for the α particle to tunnel through the Coulomb barrier starting from the daughter-α touching configuration is given by

$$T_L = \frac{\rho}{F_L^2(\eta,\ \rho) + G_L^2(\eta, \rho)}, \tag{A7}$$

where $\rho = R_0 k$ with $k = \sqrt{2\mu Q_\alpha}/\hbar$ (μ is the reduced mass) and $R_0 = 1.2(A_D^{1/3} + A_\alpha^{1/3}) + 0.63$ fm, and $\eta = 1/ka$ where $a = \hbar^2/(e^2\mu Z_D Z_\alpha)$. Here, F_L and G_L are the regular and irregular Coulomb functions [40], which take into account the additional centrifugal barrier when the orbital angular momentum L of the emitted α particle is nonzero. In the case of ground-state–to–ground-state α decay of even-even nuclei, $L = 0$.

[1] R. D. Macfarlane and A. Siivola, Phys. Rev. Lett. **14**, 114 (1965).
[2] K. Auranen *et al.*, Phys. Rev. Lett. **121**, 182501 (2018).
[3] S. N. Liddick *et al.*, Phys. Rev. Lett. **97**, 082501 (2006).
[4] D. Seweryniak, K. Starosta, C. N. Davids, S. Gros, A. A. Hecht, N. Hoteling, T. L. Khoo, K. Lagergren, G. Lotay, D. Peterson *et al.*, Phys. Rev. C **73**, 061301(R) (2006).
[5] Z. Janas *et al.*, Eur. Phys. J. A **23**, 197 (2005).
[6] L. Capponi *et al.*, Phys. Rev. C **94**, 024314 (2016).
[7] R. D. Page, P. J. Woods, R. A. Cunningham, T. Davinson, N. J. Davis, A. N. James, K. Livingston, P. J. Sellin, and A. C. Shotter, Phys. Rev. C **49**, 3312 (1994).
[8] D. Schardt *et al.*, Nucl. Phys. A **326**, 65 (1979).
[9] D. Schardt, T. Batsch, R. Kirchner, O. Klepper, W. Kurcewicz, E. Roeckl, and P. Tidemand-Petersson, Nucl. Phys. A **368**, 153 (1981).
[10] D. De Frenne and A. Negret, Nucl. Data Sheets **109**, 943 (2008).
[11] F. Heine, T. Faestermann, A. Gillitzer, J. Homolka, M. Köpf, and W. Wagner, Z. Phys. A **340**, 225 (1991).
[12] C. Mazzochi *et al.*, Phys. Lett. B **532**, 29 (2002).
[13] G. Gamow, Z. Phys. **51**, 204 (1928).
[14] R. W. Gurney and E. U. Condon, Nature (London) **122**, 439 (1928).
[15] R. G. Lovas, R. J. Liotta, A. Insolia, K. Varga, and D. S. Delion, Phys. Rep. **294**, 265 (1998).
[16] C. Qi, R. J. Liotta, and R. Wyss, Prog. Part. Nucl. Phys. **105**, 214 (2019).
[17] D. E. Ward, B. G. Carlsson, and S. Åberg, Phys. Rev. C **88**, 064316 (2013).
[18] R. Id Betan and W. Nazarewicz, Phys. Rev. C **86**, 034338 (2012).
[19] M. Patial, R. J. Liotta, and R. Wyss, Phys. Rev. C **93**, 054326 (2016).
[20] D. M. Brink and R. A. Broglia, *Nuclear Superfluidity* (Cambridge University Press, Cambridge, UK, 2005).
[21] F. Barranco, R. A. Broglia, and G. F. Bertsch, Phys. Rev. Lett. **60**, 507 (1988).
[22] F. Barranco, E. Vigezzi, and R. A. Broglia, Phys. Rev. C **39**, 2101 (1989).
[23] F. Barranco, G. Bertsch, R. Broglia, and E. Vigezzi, Nucl. Phys. A **512**, 253 (1990).
[24] R. M. Clark, H. L. Crawford, A. O. Macchiavelli, D. Rudolph, A. Såmark-Roth, C. M. Campbell, M. Cromaz, P. Fallon, C. Morse, and C. Santamaria, Phys. Rev. C **99**, 024325 (2019).
[25] J. Rissanen, R. M. Clark, A. O. Macchiavelli, P. Fallon, C. M. Campbell, and A. Wiens, Phys. Rev. C **90**, 044324 (2014).

[26] R. M. Clark and D. Rudolph, Phys. Rev. C **97**, 024333 (2018).
[27] B. Buck, A. C. Merchant, and S. M. Perez, Phys. Rev. Lett. **65**, 2975 (1990).
[28] NNDC, Evaluated Nuclear Structure Data File, http://www.nndc.bnl.gov/ensdf/.
[29] A. Bohr and B. Mottelson, *Nuclear Structure* (Benjamin, New York, 1975), Vol. 1.
[30] S. A. Changizi, C. Qi, and R. Wyss, Nucl. Phys. A **940**, 210 (2015).
[31] P. Vogel, B. Jonson, and P. G. Hansen, Phys. Lett. B **139**, 227 (1984).
[32] G. Royer, Nucl. Phys. A **848**279 (2010).
[33] R. M. Clark, A. O. Macchiavelli, L. Fortunato, and R. Krücken, Phys. Rev. Lett. **96**, 032501 (2006).
[34] P. Ring and P. Schuck, *The Nuclear Many-Body Problem* (Springer-Verlag, New York, 1980), p. 233.
[35] S. Frauendorf and A. O. Macchiavelli, Prog. Part. Nucl. Phys. **78**, 24 (2014).
[36] A. O. Macchiavelli, P. Fallon, R. M. Clark, M. Cromaz, M. A. Deleplanque, R. M. Diamond, G. J. Lane, I. Y. Lee, F. S. Stephens, C. E. Svensson *et al.*, Phys. Rev. C **61**, 041303(R) (2000).
[37] N. Sandulescu, D. Negrea, and D. Gambacurta, Phys. Lett. B **751**, 348 (2015).
[38] R. R. Betts, Phys. Rev. C **16**, 1617 (1977).
[39] R. A. Broglia and A. Winther, *Heavy Ion Reactions* (Addison-Wesley, New York, 1991).
[40] R. Thomas, Prog. Theor. Phys. **12**, 253 (1954).